Cycloidal Geartrain In-Use Efficiency Study

Logan C. Farrell[1], James Holley[2], William Bluethmann[3], and Marcia K. O'Malley[4]

***Abstract*— Currently, harmonic drives are the go-to speed reducer for robotic applications where a high reduction in a small package is required. Cycloidal drives have the ability to customize a high reduction drive that can carry high torque in a small package. These compact style cycloidal drives have been well studied in theory and simulation for their performance, but very little data is available on their actual performance over time. This paper presents experimental data on performance of a cycloidal drive designed for a robotic application. Burn-in time efficiency curves, and efficiency profiles over time are computer after running the drive through 51K output cycles (3M input cycles) over the course of 111 hours of testing. The study finds that substantial burn-in time may be required for steady-state performance, but peak efficiencies of 77% can be achieved. Also, the efficiency is shown to be dependant on the torque through the actuator. This work demonstrates a customized cycloidal drive in a robotic application that is comparable to a harmonic drive in performance, suggesting the application of cycloidal drives could grow tremendously in robotic designs.**

I. Introduction

As robotic applications flourish in our modern world, there is an increasing need for high reduction, high torque, and low backlash actuator systems. These actuators are present in all types of robotic equipment and are critical in space flight applications as well. A notable recent example includes the Curiosity rover from NASA's Jet Propulsion Laboratory that uses 33 separate motors with various reductions [**?**]. Currently, harmonic drives are the primary reduction method when high ratio and compact design are required. These reducers come in limited reduction ratio options, and can grown quite heavy to withstand the high torque applications. Ideally, one would be able to specify a desired reduction ratio and realize it in a compact, lightweight package.

A. Cycloidal Drive Motivation

Cycloidal drives are potentially an apt replacement for these harmonic drives as they can offer large a large reduction in a small package. In situations where small backlash is acceptable, cycloids offer distinct advantages. They can be customized into the system directly and are made of relatively easy to manufacture parts. In addition, the torque to weight ratio typically higher for cycloidal drives of this style. For example, the cycloid presented in this work is 2.5kg, including all housing components while a comparable harmonic drive is 5.1kg. Despite these desirable features, there is insufficient data available to quantify the true efficiency and characteristics of these drives.

The primary contribution of this research is to quantify the efficiency of a cycloidal drive system through an extended drive cycle test for burn-in to steady state performance over 51K output revolutions through over 100 hours and efficiency testing over the torque and speed range of this system.

B. Cycloidal Drive Background

Cycloidal drives were proposed as early as 1956 by Botsiber and Kingston [**?**]. The premise of this design leverages a plate, referred to as the wobble plate, with lobes interacting with pins in the housing designed using trochoidal motion being spun on an eccentric shaft with a bearing. This induces a counter-clockwise motion of the plate that is harnessed with the interior pins as the output of the mechanism (seen in Fig 1). This geartrain design has been used in industry for high torque, high shock load applications for many years including companies like Natbesco Motion Control. However, in many of these applications, all of the interacting surfaces like the housing pins and output pins use needle roller bearings to transmit load. This allows for higher efficiency and load carrying capability, but it also increases mass and volume. In the robotic industry, groups are striving to reduce the mass and volume of these actuators while still achieving high reduction and load capabilities, by eliminating many of the rolling elements at the interaction points between the wobble plate, housing pins, and output pins. This allows for very compact and strong designs to be considered, but leaves the potential for larger losses and shorter system lifetime.

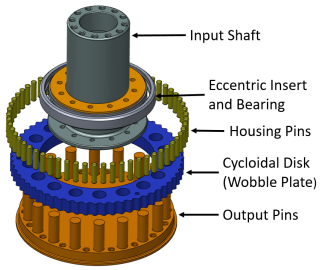

Fig. 1: Simple rendering of the key elements that create a cycloidal drive. A drive shaft spins a cycloidal disk (wobble plate) via an eccentric circle. The wobble plate reacts against the housing pins to create a counter-rotation, harnessed by the output pins.

[1]Logan Farrell is with the Department of Mechanical Engineering at Rice University and NASA: Johnson Space Center. Logan.C.Farrell@NASA.gov

[2]James Holley is with the Department of Mechanical Engineering at Rice University and NASA: Johnson Space Center.

[3]William Bluethmann is the project manager for rovers at NASA: Johnson Space Center.

[4]Marcia O'Malley is on the Faculty in the Department of Mechanical Engineering, Rice University, Houston, TX

Many works have been presented on the subject of the theoretical design of these cycloidal drives [**?**] [**?**], designing with machine tolerances [**?**], contact and stress analysis [**?**], and performance characteristics such as torque ripple and backlash [**?**] [**?**] as will be presented in Section II. These works lay a solid foundation for a designer, providing the equations and design considerations for a cycloid. Still, there is a need to present in-use characteristics to support the theoretical calculations and models.

Theoretical cycloid efficiencies have been reported in the 88-98% range [**?**], [**?**]. More recently, Sinsinger and Lipsey reported experimentally determined efficiencies for fused roller designs (42.3%) and pin designs (71%) based on 80 minutes of run-time [**?**]. The distinction between a fused roller and pin design comes in the design of the housing. In a fused design, the housing lobes are part of the housing, and in a pin design, pins are inserted the ride in the housing, allowing relative motion.

Hsieh verified the stress present in the drives in simulation and in use and demonstrated lower stress levels and torque ripple when using fused rollers [**?**].

These two results leave an open trade to designers if stress and torque ripple need to be minimized versus efficiency maximized.

The aim of this work is to utilize a custom cycloid design for a NASA rover application and show the in-use efficiency characteristics over an extended duration test. The actuator design is presented in Section II. A description of the experimental setup and procedure is provided in Section III. Finally, the results and analysis of this high torque actuator and its implications are presented and discussed in Section IV and Section V.

II. Cycloid Design

In 2007 and 2008, NASA developed a manned rover prototype for planetary surfaces for future missions [**?**]. This robotic vehicle is made up of six independent wheel modules, each with their own propulsion, steering, and both active and passive suspension. In 2014, a new prototype wheel module was designed and created to analyze potential technologies that could be used in these applications. In the new design layout, it was possible for the propulsion wheels to counter-rotate against the steering and put large shock loads into the steering system. These requirements for a high load, compact package, high shock load, and tolerance of backlash lent themselves to the selection of a cycloidal drive for the steering actuator. The prototype wheel module layout can be seen in Fig 2.

Based on the load cases, the actuator was required to output a stall torque of 2,440 Nm (1800 ft-lb) with a max output speed of 1.57 rad/s (90 deg/s) at 1,626 Nm (1200 ft-lb). The required torque/speed data points are presented in Table I with an assumed loss of 88% chosen based on the available literature. The actuator layout for the vehicle placed the motor and cycloid off center of the steering axis with an additional 5:1 reduction into the steering column,

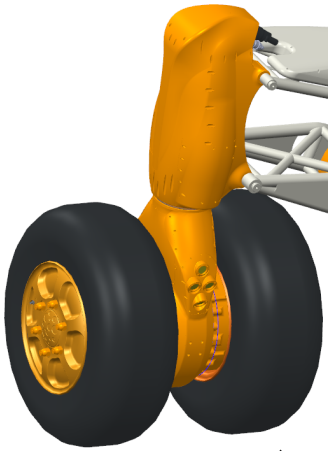

Fig. 2: CAD model of rover wheel module prototype. Suspension arms hold the steering column. Each wheel has an in-wheel propulsion motor.

thus decreasing the torque needed for the cycloid output, but increasing the potential shock loading.

Many sources have laid out the design parameters for these drives and the equations are provided below for completeness. Shin and Kwon [**?**] presented the mathematical definition of the cycloid profile as

$$C_x = Rcos\phi - R_r cos(\phi + \psi) - ecos((Z_1 + 1)\phi) \quad (1)$$

$$C_y = -Rsin\phi + R_r sin(\phi + \psi) + esin((Z_1 + 1)\phi) \quad (2)$$

$$\psi = tan^{-1}[\frac{sin(Z\phi)}{cos(Z\phi) - R/(e(Z + 1))}] \quad (3)$$

where φ is the angle of the input shaft and ψ is the angle of contact between the outer pin and the cycloid lobe.

Using both the formula for the reduction in diameter of the cycloid disk to account for machine tolerances [**?**] [**?**] as well as Ye et al.'s formula for calculating the limit of undercutting [**?**], the allowable sizes of the profiles and pins can be determined. Sensinger [**?**] laid out simple equations for calculating stress on the lobes and pins that has been further modelled and studied by others. The force on the cam for calculating the bearing load with eccentricity e, ratio Z , and torque T is

$$F_{cam} = \frac{T}{eZ}. \quad (4)$$

The simplified stress equations where *R* and R_r are defined above, *t* is the contact thickness, and *b* is the width of contact determined by (7) and (8) are

$$F = \frac{T}{R - R_r} \quad (5)$$

$$\sigma = \frac{2F}{\pi bt}(3 + 4v^2) \quad (6)$$

$$b = \sqrt{\frac{4F(v - v_1^2)/E_1 + (1 - v_2^2)/E_2}{\pi l(1/R_1 + 1/R_2)}} \quad (7)$$

TABLE I: Designed Duty Cycles for System

Time Used	Output Torque (Nm)	Output Speed (RPM)	Actuator Torque (Nm)	Actuator Speed (RPM)
5%	2440	6.8	554.7	33.9
20%	1627	6.8	369.8	33.9
60%	542	15.3	123.3	76.3
15%	135	15.3	30.8	76.3

$$R_2 = \frac{(R - eZ - e)^3}{R - e(Z-1)^2} - R_r. \tag{8}$$

The stress calculations and trading of overall size and ratio led to a necessary plate thickness of 3.81cm (1.5in) ((TODO: Verify). Instead of a single large plate however, three wobble plates were selected to split the load on the central input shaft across three bearings as well as to build in natural balance for the actuator. If a single plate is used, a counterbalance must be added to avoid extreme vibration. In this case, the three plates were offset 120° to balance these loads and vibration. This adds additional stack height to the system to allow separation between the plates. This arrangement allows the large design loads to be able to be handled by the system. The exploded view of this design can be seen in Fig 3.

The actuator uses a Parker Frameless Kit Motor, model K089200-7Y with no hall effect sensors and is commutated using a Renishaw RM-44 magnetic incremental and absolute position sensor. The final reduction is 59:1 going before into the final 5:1 output gear. The system is commutated using the delta hysteresis commutation scheme [**?**] using velocity control.

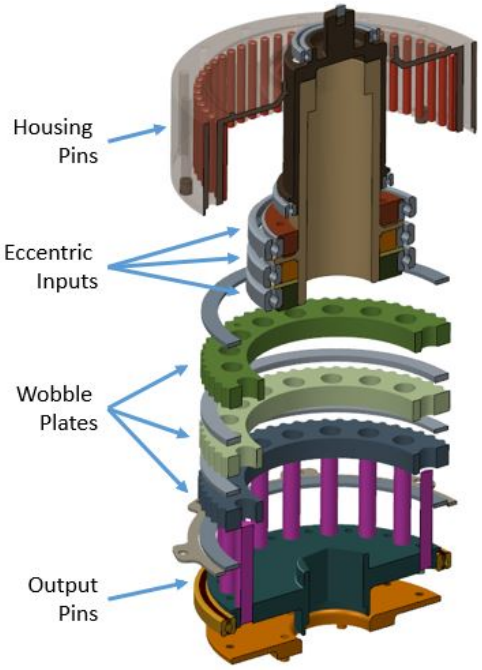

Fig. 3: Exploded view of the cycloidal reducer. Three wobble plates are driven by the input shaft with 120° offsets. The ring pins are are free pins inserted in the housing. The output has pins that run through all three wobble plates to harness the counter-rotation for the drive output.

III. Experimental Methods

The authors sought to experimentally determine and compare the cycloidal drive in-use efficiency results to the published performance data for a comparable harmonic drive.The test setup is shown in Fig 4. The actuator is mounted directly to a Futek TF600 5000inlb load cell to measure direct output torque of the actuator. This is read through a load cell conversion board into the motor driver. A verification of torque readings was completed using a calibrated torque wrench to ensure accuracy of the conversion. The motor output runs through a 36:1 (TODO) speed increase via three chain stages that then inputs into a Magtrol HB-1750 hysteresis brake that is powered using a separate 24V Lambda-TDK power supply controlled by the computer. The motor is driven with a custom motor driver powered from a 12V Lambda-TDK power supply for logic power, and a 300V, 5A TDK-Lambda power supply for motor power. The motor is commutated using the incremental encoder and an index pulse and is reading the RMS phase current, motor and bridge temperatures with thermistors, motor velocity, and the torque measurement from the custom conversion board. These values are then streamed to a controlling computer

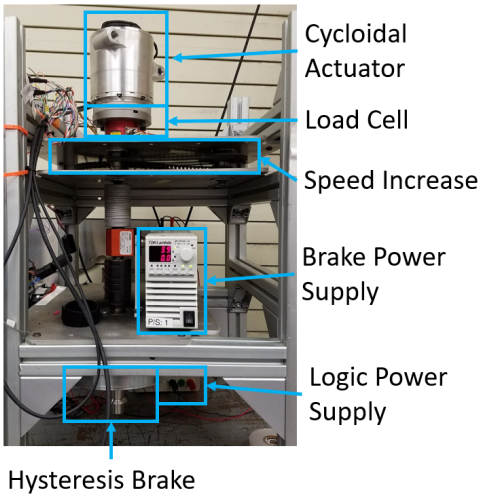

Fig. 4: Experimental Test Setup. The cycloid actuator is mounted to structure via the load cell. There is a speed increase so the brake can generate enough torque on the system. Not pictured is the controlling computer, motor driver, and high voltage supply.

that is also monitoring the high voltage supply and recording voltage and current to determine input power to the system.

Due to the tightly integrated actuator design, the motor and cycloid cannot be separated to purely isolate the losses in the cycloid. The efficiency map of the motor over its torque and speed range was provided by Parker Motors. For calculation purposes, this table is used as a lookup table for efficiency of the motor given the current motor velocity and rms input current. While this does generate a level of uncertainty in the data, these motors are mass manufactured and defects are assumed to be small. Therefore, the error in the motor efficiency map is assumed to be small and would not influence the perceived trends and results. The efficiency losses in the motor driver can be characterized primarily by the TODO – switching electronics and which are rated as 97% efficient in this voltage and current range – TODO.

The system was tested in two separate ways, an efficiency cycle and a long term drive cycle. The efficiency cycle test was run after the long term drive cycle to ensure steady state performance before cycling through a set of velocities and torques. The actuator is subjected to eight velocity steps increasing 0.25 rad/s each time. In each velocity step, the torque is ramped up and maintained for 15 seconds at values of 1Nm, 15Nm, 52Nm, 94Nm, and 189Nm. This testing profile can be seen in Fig 5. The long term drive cycle was run continuously each day for 6 to 12 hours with the duty cycles shown in Table II. The total runtime of the system not including the initial checkout and verification of the actuator has been 111 hours.

It should be noted that the actuator was used briefly in the robot validation after initial development and construction of the prototype wheel module. The total time of use was approximately three hours. Afterwards, it was removed from the wheel module and subjected to the individual testing that is discussed in this work. The motor has a continuous current

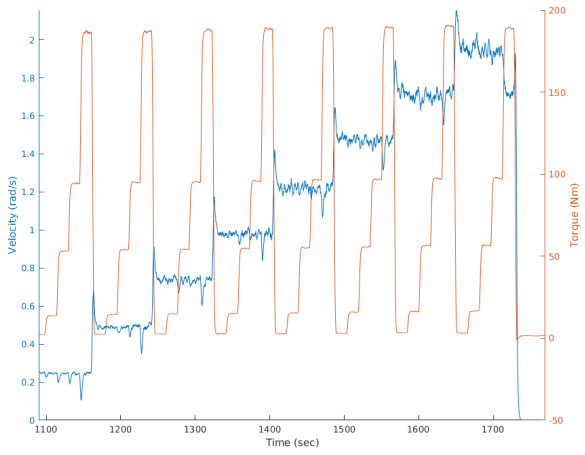

Fig. 5: Testing profile for efficiency. At each speed step, torque is ramped up through five different levels, then the speed is increased. At the last step, the maximum of the supply was reached so motor velocity dropped.

TABLE II: Long Run Drive Cycle

Time (s)	Velocity (rad/s)	Torque (Nm)
150	1.0	0.0
150	-1.0	0.0
60	0.5	26.0
60	-0.5	26.0
150	1.5	10.0
150	-1.5	10.0
30	1.0	50.0
30	-1.0	50.0
300	0.5	18.0
300	-0.5	18.0

rating of 4.3 A_{rms} and a peak rating of $15A_{rms}$. The actuator was designed to be fluid cooled to allow operations above the continuous values, but this could not be achieved during testing. For long duration testing, the torque values were decreased to avoid thermal issues. The motor was tested to approximately $6A_{rms}$ during efficiency testing due to the limit of the power supply. Also, the motor driver's rated limits are 150V, therefore the actuator's maximum rated speeds could not be attained. The nominal cycle of the actuator as seen in Fig I is still achievable and has been tested.

IV. Results

Duty cycle testing was first performed on the actuator. These tests were done at lower torques to prevent the motor from overheating to allow extended duration testing. The total test time prior to these duty cycle tests was approximately 5.2 hours to bring up and check out the actuator testbed system. Once this checkout was complete, the 100 hours of duty cycle testing were conducted the course of 11 days with the drive cycle discussed in Section III. Three of the torque/speed combinations in forward and reverse are plotted on Fig 6 to show the general characteristic trends seen in actuator performance.

After this duty cycle testing to ensure the actuator had sufficiently broken-in and achieved steady state performance, the pure efficiency cycles were run. As discussed in Section III, a profile of speeds and torques were run on the actuator to show the relationship between speed, torque, and efficiency. An example of this profile can be seen in Fig 5. This profile was run three times and the results at each torque and speed combination were averaged (see Fig 7.

V. Discussion

The efficiency of the system is dependant on the torque through the gearbox as shown in Fig 7. This contradicts previous studies that suggested that cycloidal drives have a constant efficiency across the torque range. There is also a much less pronounced relationship between the velocity and the cycloid efficiency that can be noted in the torque bands. This result suggests that the cycloid efficiency behaves more like a planetary or harmonic drive gearbox in its efficiency profile. A comparison of cycloid, harmonic, and planetary efficiency profiles can be seen in Fig 8. The figure shows the efficiency for a harmonic drive CSG-50-80-2UH [**?**] which

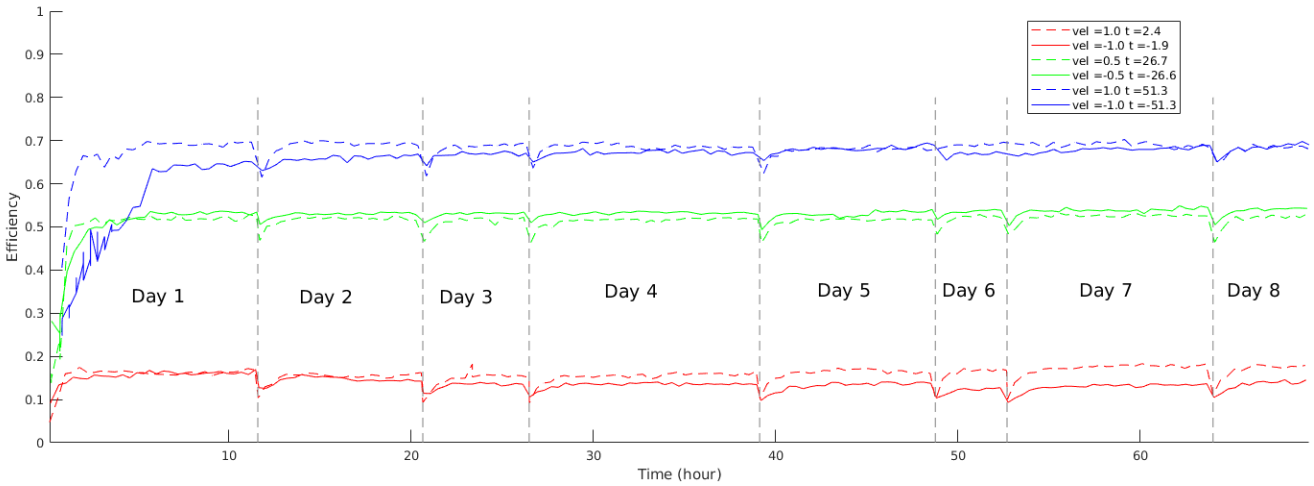

Fig. 6: Efficiency over time for three different speed/torque profiles during the drive cycle. The forward motion can be seen with the dotted line, reverse with the solid line. At the onset of testing, visible efficiency gains are made. As each day begins, there is a clear warm-up period before steady state. TODO: add a line for start of each day

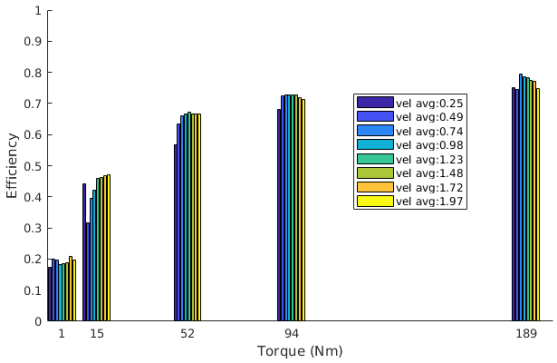

Fig. 7: Grouping of average efficiencies at each torque step. Efficiency depends heavily on torque, and slightly on speed.

has a comparable ratio and torque capability to the tested cycloid and weighs 19.5kg, and a representative planetary efficiency curve from the engineers at Maxon Motor. This shows that if backlash is acceptable in the system, a cycloidal drive can provide similar or better efficiency profiles to a harmonic drive while providing a potential 2x increase in torque density.

From Fig 6 it can be observed that there was a substantial break-in time for the actuator before steady state results were achieved. In the high torque case, specifically in the reverse direction, there was an approximately linear increase in efficiency over the course of the first seven hours of duty cycle testing. This testing began after a minimum of five hours of run time spread out through many short sessions while getting the test system running. The large increase in efficiency can be noted in the other lower torque profiles as well, starting well below their final steady state values. The authors theorize that this is potentially due to break-in of the manufactured parts due to machining inaccuracies. Due to the complex interaction required of the trochoidal motion profile, slight manufacturing deficiencies could cause build-ups of stress and loss in particular points on the drive. It would make sense that these could manifest in one direction and not the other if a lobe was misshapen on the trailing edge in one direction, it would be the lead in the other, causing the additional loss. Through the first hours of testing, these materials likely wore in to each other until the contact was smooth, resulting in the more readily achieved steady state efficiencies.

Additionally, there is a marked improvement over the first 30 minutes of runtime in the efficiency of the system. This is likely due to the grease and heat in the system. The gearbox is greased with Lucas Oil Red'N'Tacky[1] which has a viscosity index of 86 min. This was chosen because it

[1] https://lucasoil.com/products/grease/red-n-tacky-grease

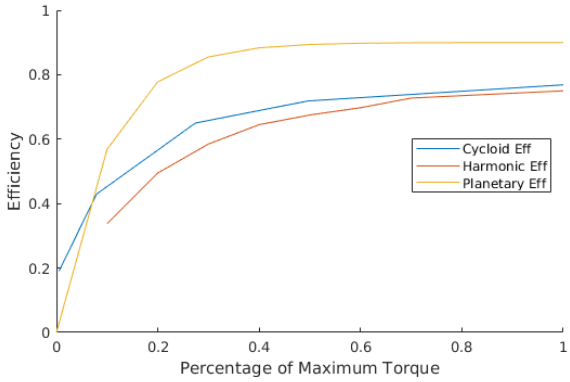

Fig. 8: Comparison of efficiency over maximum torque rating of the tested cycloid, a comparable harmonic drive, and a theoretical planetary gearset. The cycloid exhibits the same efficiency increase over torque range and has a comparable and slightly higher efficiency than the harmonic.

is designed for high loads for extended periods of time in gear and sliding surface applications. Therefore, during the warm-up period as the actuator temperature increases, the viscosity decrease is likely enough to cause a notable increase in efficiency of the system. The authors leave the study of a lower viscosity grease's effect on performance for future work.

VI. Conclusion

This study demonstrates a cycloidal actuator with a ratio of 59:1 and three phased cycloid disks that achieves a maximum efficiency of 77% and does not show a constant efficiency through its torque profile as suggested by previous sources. This research shows that these drives efficiencies behave very similarly to other typical reduction drives for similar applications like Harmonic Drives and Planetary gears. This actuator compares closely to its Harmonic Drive counterpart in efficiency performance. If backlash is acceptable in the system, a cycloidal drive has the distinct advantage of being customized into the housing using simple manufacturing techniques allowing tighter integration into a robotic system as well as a potential 2x torque density gain. An item of interest that has not been characterized by the community is the lifetime characteristics of these actuators and this is left by the authors for future work. Cycloidal drives of this design style are quite comparable to similar use-case drives and should be considered in high reduction applications.

VII. Acknowledgements

The authors would like to thank the original actuator designer, Mason Markee for his support in the testing and research of this system.